International Journal of Thermal Sciences 49 (2010) 365–372

Contents lists available at ScienceDirect

International Journal of Thermal Sciences

journal homepage: www.elsevier.com/locate/ijts

A predictive model for the evolution of the thermal conductance at the casting–die interfaces in high pressure die casting

A. Hamasaiid [a,*], G. Dour [a], T. Loulou [c], M.S. Dargusch [b]

[a] Université de Toulouse, INSA, UPS, Mines Albi, ISAE, ICA (Institut Clément Ader), CROMeP, Campus Jarlard, F-81013 Albi Cedex 09, France
[b] CAST Cooperative Research Centre, School of Engineering, The University of Queensland, St. Lucia, Brisbane QLD 4072, Australia
[c] Université de Bretagne-Sud, LIMAT B, rue de Saint-Maudé, 56321 Lorient, France

ARTICLE INFO

Article history:
Received 15 January 2009
Received in revised form
18 June 2009
Accepted 15 July 2009
Available online 4 August 2009

Keywords:
Thermal contact resistance
Heat transfer coefficient
Thermal conductance
High pressure die casting
Solidification

ABSTRACT

An analytical model is proposed to predict the time varying thermal conductance at the casting–die interface during solidification of light alloys during High pressure Die Casting. Details of the topography of the interface between the casting and the die are included in the model through the inclusion of solid surface roughness parameters and the mean trapped air layer at the interface . The transitory phase of the interfacial thermal conductance has been related to the degradation of contact as solidification progresses through the casting thickness. The modelled time varying thermal conductance showed very good agreement with experimentally determined values for different alloy compositions and casting geometries. The analysis shows that the parameters that govern the thermal conductance are different for the first stage of contact compared to the second stage of contact when the alloy begins to solidify.

1. Introduction

High Pressure Die Casting (HPDC) is a cyclical manufacturing process suitable for the production of large numbers of low cost components requiring high dimensional accuracy and complex geometry. In HPDC the molten metal is injected into the die with extremely high velocity (50–60) ms^{-1} followed by the application of an intensification pressure (300–1000 bar) after the cavity filling process is complete. This intensification pressure is applied in order to minimise the porosity in the casting and to eliminate the effects of contraction in the solidified casting [1]. It is maintained until the complete solidification of the molten metal in the die. The heat is primarily removed from the cast molten metal through the casting–die interface and die blocks into the cooling medium, until solidification of the casting is complete. Shortly after solidification, the casting component is removed from the die. This process results in the production of a uniform component with generally good surface finish and good dimensional accuracy (±0.2%).

Even though the HPDC process was invented (in its preliminary form) about a century ago, the scientific investigations seeking to improve the various aspect of this process are quite recent since much of the focus has previously been on the development of the hydraulic, mechanical and control systems of the machine. It is only over the last two decades that investigations of this process have become increasingly important. There have been some publications relating the quality of the produced component to solidification conditions along with the heat transfer [2–8] Research issues associated with tooling such as thermal fatigue and chemical reaction between the die and the casting during solidification has also become an increasingly important commercial issue as the relatively short lifetime and the effective cost of the die play an important role in the determination of the final cost of production.

The extreme complexity of experimental trials in a high pressure die casting environment and the associated costs along with the technical limitations inherent in the process, mean that development of predictive tools to simulate various aspects of the manufacturing process such as die filling, solidification, thermal conditions of the die and subsequently die life for different die and casting compositions is a high priority for the industry. Today, the commercial softwares that simulate the filling stage in HPDC is available and the have been considered reliable by industries. Nevertheless, the most important stage (solidification) and the associated heat transfer from the casting to the die is rarely modelled.

A detailed knowledge of the solidification environment (cooling rate, solidification path, and the cooling down of the casting) is an

* Corresponding author. Tel.: +33 5 63 49 32 95; fax: +33 5 63 49 32 42.
E-mail address: hamasaii@mines-albi.fr (A. Hamasaiid).

1290-0729/$ – see front matter © 2009 Elsevier Masson SAS. All rights reserved.
doi:10.1016/j.ijthermalsci.2009.07.014

Nomenclature

a_s	radius of microcontacts, m
C	constant which characterises the layer of the solidified alloy
f_s	solid fraction
h, h_0	heat transfer coefficient, W m^{-2} K^{-1}
L	latent heat, J/kg
n_s	density of microcontacts, m^{-2}
P_1	pressure in the melt in the vicinity of the rough surface, Pa
$P(\gamma)$	pressure due to the surface tension of liquid, Pa
q, q_{max}	heat flux density and its peak value, Wm^{-2}
R_a	arithmetic average of the absolute values of the measured profile height deviations, m
R_q, σ	square root of the average of the square of the deviation of the profile from the mean line, m
R_{sm}	mean peak spacing, m
R_s	thermal constriction and spreading resistance, K/W
S_t	overall thickness of the casting, m
R	thermal contact résistance, m^2 K/W
T_0	initial air temperature, K
Tm_0	initial die temperature, K
T	temperature, °C
T_M	alloy pouring temperature, K.
Y	mean surface plane separation (mean trapped air thickness), m
V_{al}	volume of they alloy penetrated into the microcavities, m^3

Greek symbols

γ	surface tension of metal liquid, N/m
ρ_s	density of solid phase of casting, kg/m^3
λ	thermal conductivity, W m^{-1} K^{-1}
$\varphi(y)$	Gaussian (normal) distributions function of the asperity heights
ΔT	temperature difference at the interface, K
σ	standard deviation of the asperities heights, m

essential element in the development of any predictive model. Using the optimum set of process parameters such as filling velocity, die cooling rate, pressure are linked indirectly to the solidification mechanisms. Besides, it is well known that the solidification rate is governed by the rate of the heat transfer at the casting–die interface during solidification [9]. This is characterised by the value of the thermal conductance or heat transfer coefficient at the casting–die interface. Hence, in HPDC, the process efficiency and the microstructural features of the produced castings are strongly dependent on heat transfer through the casting–die interface during solidification [10,11].

It has been reported in the previous publications of our research group [12–15] that the heat transfer could be affected by number of the process parameters such as piston velocity, die temperature, casting thickness and also by the casting–die interface properties. Nowadays, non of the commercialized simulation software for die casting take into account the time and process parameters dependence of the interfacial heat transfer during HPDC because of the absence of meaningful information in this area. Thus, considering the role that heat transfer has during solidification in HPDC, the effectiveness of the simulation work is limited. Therefore, modelling and measuring the variation of heat transfer processes with time and process parameters is presently a key requirement for further development of the HPDC process simulation.

The present paper deals with an analytical predictive model for the time varying thermal conductance during casting and solidification of the metallic alloys in HPDC process. In the present paper, we will mention and discuss thermal contact conductance (h) rather than thermal contact resistance as this term is more commonly used by the chief investigators in the field.

2. Theoretical approach

2.1. Modelling of the initial thermal conductance

It is known that the die surface is rough at a microscopic scale. The typical values of the roughness parameter, Ra, of the high pressure die vary between (0.2 μm to 5 μm) depending on die life and surface machining methods. When the cast liquid contacts the die surface, an amount of air is entrapped between the surface of the cast liquid and the die surface [16–20], typically, inside the micro-cavities of the asperities. The only real contact occurs at the areas around the top of the asperities and this is a small fraction of the apparent contact area [20] as illustrated in Fig. 1. The heat flux is then constricted by this interface and can only pass through these real contact areas at the top of the asperities. This constriction of heat flux leads to a temperature jump at the interface that characterises the Interfacial Thermal Constriction Resistance (R) by the following relationship:

$$R = \frac{\Delta T}{q} \tag{1}$$

The interfacial thermal conductance is simply the inverse of R.

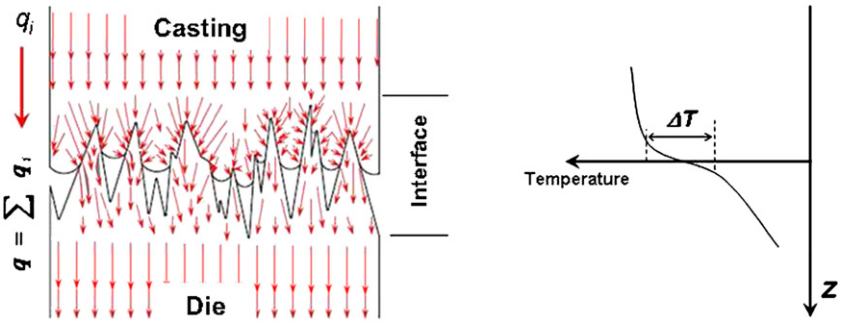

Fig. 1. Schematic of the casting liquid–die contact (vertical scale exaggerated) showing the constriction of the heat flux as it passes through the microcontact area at the interface and the temperature profile at the interface.

Accurate modelling of R depends on an accurate characterisation of the casting–die contact topography. When the liquid casting contacts the die surface, air is expected to be entrapped at the bottom of the microcavities of the die surface. The bottom levels of the microcavities of the die surface are randomly situated and distributed as shown in Fig. 1. They have to be considered while modelling R at the casting liquid–die interface because they quantify the entrapped air volume hence the quality of contact between the casting and die surface.

In practice, the solid surface heights and distribution are generally expressed in a format as measured by profilometers. Profilometers characterise the solid surfaces from a mean plane where the standard deviation of the heights is minimised reference [21]. From the definition of Ra (Equation (2)) for a Gaussian surface, one can note that the bottom microcavities can be considered in fact as asperities. Using this definition, one can not quantify reasonably the entrapped air while describing the topography of the casting.

$$R_a = \int_{-\infty}^{+\infty} \phi(y)|y|\mathrm{d}y \tag{2}$$

Therefore, we propose to modify the surface profile of the solid to have a common base as illustrated in Fig. 2. The summits are supposed to be conical in shape with a similar normalised slope (m_n) and height distribution. Then there are no more valleys or in other words the valleys have been brought at the same level ($y = 0$). For this new equivalent die surface profile, we have to ensure that the profile characteristics (R_a, R_q, R_{sm}) measurable by profilometers remain representative of the new surface profile. In order to achieve this, we propose that the height (y) distribution of the peaks for the normalised surface follow a new distribution $\phi_B(y)$ function derived from Gaussian function which is expressed by Equation (3):

$$\phi_B(y) = \frac{2}{\sqrt{2\pi\sigma}}\exp\left(\frac{-y^2}{2\sigma^2}\right) \quad \forall y \in \{0, +\infty\} \tag{3}$$

Fig. 2 shows the normalised die surface profile and the plot of its distribution function, and $\phi_B(y)$ compared to the real surface profile and the Gaussian distribution functions $\phi(y)$ The main feature of $\phi_B(y)$ is that it applies uniquely for $y > 0$ and it is double the value of $\phi(y)$ in the domain of validity.

Then, the new definition for the arithmetic average of the modelled profile becomes

$$< y > = \int_{y=0}^{y=+\infty} \phi_B(y) y \,\mathrm{d}y = \int_{y=-\infty}^{y=+\infty} \phi(y)|y|\mathrm{d}y = R_a \tag{4}$$

Therefore, the measurable parameters (Ra, Rq and Rsm) which characterise the die surface profile remain representative of the normalised surface profile.

With this normalised die surface profile, the casting–die contact topography can be also normalised as shown in Fig. 3. The asperities whose heights are above Y make contact with the liquid surfaces while the smaller peaks do not. In other words, the mean separation plane Y defines the density of the microcontact spots and the constriction between the projected diameter of the microcontact points ($2a_s$) and the projected diameter of the cone bases ($2b_s$). Then the density of the microcontact area at Y can be given as follows

$$n_s = n_{\mathrm{pic}} \int_{y=Y}^{y=+\infty} \phi_B(y)\mathrm{d}y \tag{5}$$

The solution yields

$$n_s = n_{\mathrm{pic}} erfc\left(\frac{Y}{\sqrt{2}\sigma}\right) = \frac{8}{\varepsilon\pi^2}\left(\frac{1}{R_{sm}}\right)^2 erfc\left(\frac{Y}{\sqrt{2}\sigma}\right) \tag{6}$$

The average radius of the projected contact area, a_s, for the asperities which have a height that exceeds the entrapped air thickness Y can be similarly determined from the proposed distribution function as follows:

$$< a_s > = \int_{y=Y}^{y=\infty} \frac{(y-Y)}{m_n}\phi_B(y)\mathrm{d}y \tag{7}$$

Solving this Equation gives

$$< a_s > = \frac{1}{2}\sqrt{\frac{\pi}{2}}R_{sm}\left(\frac{2\sigma}{\sqrt{2\pi}}\exp\left(-\frac{Y^2}{2\sigma^2}\right) - Y erfc\left(\frac{Y}{\sqrt{2}\sigma}\right)\right) \tag{8}$$

Based on these equations, the thermal conductance has been modelled as a function of the topography and mechanisms of contact by the following equation [22]

$$h_o = = 2\lambda_s < n_s > \frac{< a_s >}{\left(1 - \frac{2 < a_s >}{R_{SM}}\right)^{1.5}} \tag{9}$$

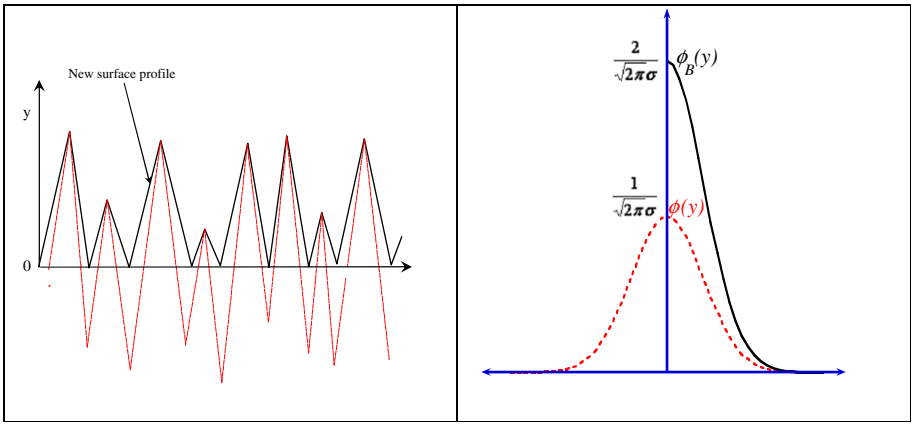

Fig. 2. Normalised surface profile equivalent to the real surface profile and the equivalent distribution function as compared to the Gaussian distribution function.

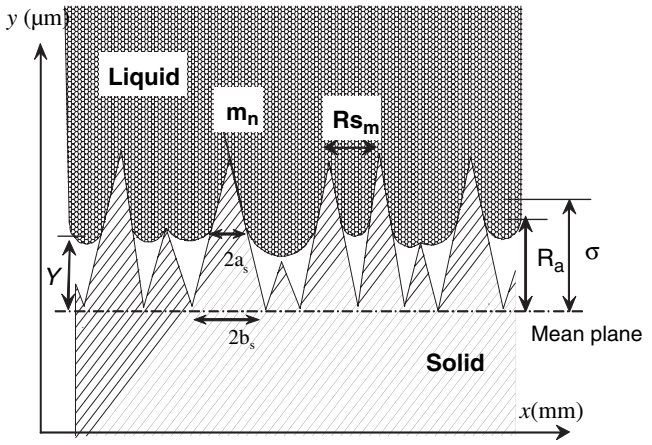

Fig. 3. Normalised profile of the casting liquid–die contact (vertical scale exaggerated). Ra is the arithmetic average of the absolute values of the measured profile height deviations, σ is RMS value and Rsm is the mean peak spacing.

The above equations show that the number and the radius of the contact spots and consequently the thermal conductance are determined by the mean separation plane, Y, (see Fig. 3) for a given casting–die interface. As for Y, it characterises the amount of air that could be entrapped during the sudden contact of the casting liquid with the die. In HPDC, during the first stage of casting–die contact when the casting is mostly liquid, Y is at its minimum value. This is because the casting liquid spreads well over the surface of the die and it can enter easily into the die surface roughness under the applied pressure. The minimum value of Y for a given casting–die contact means a maximum value for a_s and n_s according to Equations (2) and (3) which give a maximum value of h for this contact configuration.

2.2. Modelling of the variation of the thermal conductance during solidification

The experimental determination of h reported by the present authors [12,15] has shown that the value of h varies as a function of solidification time. During the first instant of contact when the casting is still liquid, the thermal conductance is at its maximum value, followed by a sharp decrease when solidification develops. If the explanation reported above (see Section 2.1) justifies the raison for the maximum value of h during the first stage of contact, the sharp decrease of h during solidification requires a profound understanding of the heat transfer and solidification mechanisms that occur during this process.

It has been reported that the drop of h at the casting–die interface in HPDC is mainly due to the degradation of contact between the casting and the die as a result of solidification [20]. It is known that when a molten alloy is brought into contact with a relatively cold die and heat is transferred from the melt to the die, nucleation and grain growth should begin at the contact areas, and more precisely, around the peaks of the asperities [20,23,24] where the melt temperature is the lowest.

In the case of HPDC, due to the large applied pressure on the casting, the number and the area of contact points are very important and produce a large maximum value for the thermal conductance at the first stage of contact, when the molten alloy is still mostly liquid. When the density of contact spots and h are large, the nucleated grains around the peak of the asperities in contact reach each other quite rapidly and form the first solidified film of the casting or casting skin near the interface, hence, the liquid–solid contact is transformed almost immediately into a situation of solid–solid contact. When the casting skin forms, the thermal gradient in the solidified film causes local shrinkage and possibly defects in the solidified component. This contraction may cause the solidified skin to partially separate from the die if the main contraction direction is perpendicular to the interface mean plane. This contraction can also be parallel to the interface mean plane. In that case the distance between the two contact spots reduces. Because of the rigidity of both solids and of the slope of the asperities, the interface necessarily moves apart, resulting in the reduction of the number and the area of the micro-contact spots. This is the main reason for the sharp drop of the h as a function of solidification time.

Based on this interpretation, the time dependence of t h should be a function of the solid fraction (f_s), and the initial value (peak value) of the thermal conductance (h_0) at the casting die interface.

$$h(t) = f(f_s(t), h_0) \tag{10}$$

As explained before, h_0 is associated with the first stage of contact when $Y = Y_0$. Then Equation (9) can be re-writing as follows:

$$h_o = 2\lambda_s n_s(Y_o)\frac{< a_s(Y_o) >}{\left(1 - \dfrac{< a_s(Y_o) >}{< b_s >}\right)^{1.5}} \tag{11}$$

As discussed previously when solidification progresses, the separation plane characterised by Y moves away from the die surface. Therefore, n_s and a_s must change. This necessarily results in a change in the value of h from its initial value. Therefore, $f(f_s(t), h_0)$ can be replaced by an equation of the type of Equation (12) in which Y is a function of fs; i.e. $h(t) = h(Y(f_s(t), h_0)$.

In an attempt to model, we propose the following relation ship for $Y(t)$:

$$Y(f_s(t)) = Y_o + Cf_s(t) \tag{12}$$

Where Y_o is the initial value of Y which can be determined from the following relationship driven from the perfect gas laws as explained in reference [25]:

$$< Y_o > = \sqrt[3]{2\frac{P_0}{(P_1 - p(\gamma))}\frac{T_1}{T_0}} \times \sqrt[6]{\frac{2}{\pi}}\sigma \tag{13}$$

We should note here that the $P(\gamma)$ accounts for surface tension back pressure due to the liquid meniscus curvature inside the micro-cavities between the peaks in contact.

The next step is to find a way to estimate the function $f_s(t)$ in Equation (12) and the factor C.

For a unidirectional heat flow problem along the x direction the heat conduction condition across a solid front is determined as follows [11]:

$$\rho L\frac{\mathrm{d}s}{\mathrm{d}t} = \lambda_s\left[\frac{\mathrm{d}T}{\mathrm{d}x}(s,t)\right]_s - \lambda_L\left[\frac{\mathrm{d}T}{\mathrm{d}x}(s,t)\right]_L \tag{14}$$

where ds/st is the velocity of the solidification front.

In the solid phase around the final eutectic solidification, thermal gradient is lower than the liquid phase as a result of the interface being the main heat transfer limitation. Therefore, the solid contribution (right side of Equation (14)) can be neglected. Then Equation (14) is transformed to equation (15).

$$\rho L\,\mathrm{d}s = q\,\mathrm{d}t \tag{15}$$

where $q = -\lambda_L[\mathrm{d}T/\mathrm{d}x]_L$.

The solidified casting thickness as a function of time can be determined by integrating Equation (15) from $t = 0$ to t as follows:

$$s(t) = \frac{1}{\rho L}\int_0^t q\,\mathrm{d}t \tag{16}$$

Then the solid fraction in the casting, $f_s(t)$ can be estimated by dividing $s(t)$ by the half of the casting thickness (S_t) as it has been assumed that the solidification is unidirectional, as follows:

$$f_s(t) = \frac{2}{\rho L S_t}\int_0^t q\,\mathrm{d}t \tag{17}$$

Substituting (17) into (12) yields

$$Y(f_s(t)) = Y_0 + \frac{2C}{\rho L s_t}\int_0^t q\,\mathrm{d}t \tag{18}$$

The above analysis is only valid if the solidification front is formed during casting solidification. This can be verified with Equation (19) that gives the order of magnitude of the mushy zone thickness (S_{mushy}) [11].

$$s_{\text{mushy}} = \frac{\lambda \Delta T}{q} \tag{19}$$

Using the experimental results reported by the present authors in [12,14,15], the numerical application of Equation (19) shows that the mushy zone is very narrow in HPDC (0.27 and 0.2 mm respectively for Al-9Si-3Cu and AZ91 D alloys) which corresponds to less than 9% of half of the total casting thickness that was used in the above mentioned references. Therefore Equation (18) can be appropriately applied in the case of HPDC.

In the very first stages of the solidification process the heat flux crossing the die–casting interface is at its highest value. When the solidification progresses, the heat flux drops down to its minimum in a very short time. The experimental results reported in [12,14,15] shows that the drop of the heat flux at earlier stage of solidification is continue as illustrated in Fig. 4. Therefore, the term $\int_0^t q\,\mathrm{d}t$ in Equation (18) can be linearised. Moreover, this earlier stage of solidification corresponds to the period when the heat transfer experiences the major variation as illustrated in Fig. 4. Therefore, it would seem reasonable to approximate this term by the following.

$$\int_0^t q\,\mathrm{d}t = h_O(T_M - T_{mO})t \tag{20}$$

Then equation (18) becomes

$$Y(f_s(t)) = Y_0 + 2Ch_0\frac{T_M - T_{m0}}{\rho L S_t}t \tag{21}$$

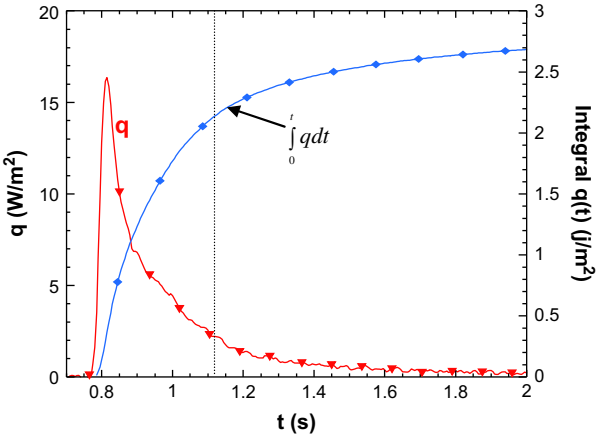

Fig. 4. Heat flux and its integration with respect to time during casting of the AZ91 D alloy in HPDC.

In this equation the constant C needs to be a distance variable. Using Vaschy–Buckingham analysis, C is expected to be related to the die surface roughness parameters such as asperities and valleys. For this raison, we assume that C is a representative constant for the valleys and peak density as the best option to estimate this constant. It is determined empirically to be the half of the averaged volume of the alloy inside the valleys of the asperities times the peak density (Equation (22)).

$$C = \frac{1}{2}V_{al} \times n_s \tag{22}$$

The volume of alloy, V_{al}, inside the asperities is determined by extracting the average volume of the entrapped air from the average volume of the valleys based on the distribution function for the modelled surface ($\phi_B(y)$) presented above.

$$V_{al} = \frac{1}{3}\pi\frac{1}{m_n^2}\int_{y=0}^{y=+\infty}\phi_B(y)y^3dy - \frac{1}{3}\pi\left(\frac{Y_0}{m_n}\right)^2\int_{y=0}^{y=Y_0}\phi_B(y)y\,\mathrm{d}y \tag{23}$$

The solution for Equation (23) yields

$$V_{al} = \frac{\pi}{3}\frac{\sigma}{m_n^2}\left[2\sqrt{\frac{2}{\pi}}\sigma - Y_0^2\frac{2}{\sqrt{2\pi}}\exp\left(\frac{-Y_0^2}{2\sigma^2}\right)\right] \tag{24}$$

Substituting (24) in (22) and then in (21) yields

$$\begin{aligned}<Y(t)> = Y_0 + &\left[\frac{\pi\sigma}{3m_n^2}<n_s(y)\right.\\ &\left.>\left(2\sqrt{\frac{2}{\pi}}\sigma - Y_0^2\frac{2}{\sqrt{2\pi}}\exp\left(\frac{-Y_0^2}{2\sigma^2}\right)\right)\right]\left(h_0\frac{T_M - T_{m0}}{\rho_s H S_t}t\right)\end{aligned} \tag{25}$$

The average of the density (n_s) and the radius of the micro-contact points (a_s) are expressed by Equations (6) and (8). Now they can be expressed as a function of time when using $Y(t)$ instead of constant Y as shown in Equations (26) and (27).

$$<n_s(t)> = \frac{4}{\varepsilon\pi^2}\left(\frac{1}{R_{sm}}\right)^2 erfc\left(\frac{Y(t)}{\sqrt{2}\sigma}\right) \tag{26}$$

$$<a_s(t)> = \frac{1}{2}\sqrt{\frac{\pi}{2}}\frac{R_{sm}}{\sigma}\left(\frac{2\sigma}{\sqrt{2\pi}}\exp\left(-\frac{Y^2(t)}{2\sigma^2}\right) - Y(t)erfc\left(\frac{Y(t)}{\sqrt{2}\sigma}\right)\right) \tag{27}$$

Combining Equations (26), (27) and (9), the thermal conductance at the casting–die interface can be expressed by the following relationship as a function of time:

$$h(t) = \lambda_s R_{sm}\left(\frac{8}{\varepsilon\pi^2}\left(\frac{1}{R_{sm}}\right)^2 erfc\left(\frac{Y(t)}{\sqrt{2}\sigma}\right)\right) \times \frac{\left(\frac{1}{2}\sqrt{\frac{\pi}{2}}\frac{R_{sm}}{\sigma}\left(\frac{2\sigma}{\sqrt{2\pi}}\exp\left(-\frac{Y(t)^2}{2\sigma^2}\right) - Y(t)erfc\left(\frac{Y(t)}{\sqrt{2}\sigma}\right)\right)\right)}{\left(\frac{R_{sm}}{2} - \left(\frac{1}{2}\sqrt{\frac{\pi}{2}}\frac{R_{sm}}{\sigma}\left(\frac{2\sigma}{\sqrt{2\pi}}\exp\left(-\frac{Y(t)^2}{2\sigma^2}\right) - Y(t)erfc\left(\frac{Y(t)}{\sqrt{2}\sigma}\right)\right)\right)\right)^{1.5}} \tag{28}$$

3. Assessing the validity of the model

The authors of the present paper have developed a new measurement method to determine, experimentally, the thermal conductance at the casting–die interface during high pressure die casting (HPDC) of light alloys. The casting surface temperature was measured using infra-red probes linked to pyrometric chain. The temperatures inside the die, at different depths from the die surface, were measured using a thermocouple arrays (ϕ 0.25 mm). The thermocouples measurements have been analysed using an inverse method in order to evaluate the heat flux density at the casting–die interface and the die surface temperature. Extra care detailed in [12,14,26] has been taken to reduce measuring errors with both pyrometer and thermocouples. Hence, the thermal conductance and its evolution during solidification of the casting are determined accurately for different casting conditions (alloy type, applied pressure, etc). In addition, the error in the *h* measurements due to the limitations in the inverse method, the dynamics of thermocouples in transient heat transfer and other deterministic uncertainties were evaluated. The details of the experimental procedure, analysis and results have been reported in reference [12,14].

The following analysis compares the reported experimental *h* in references [12,14] to the results of the numerical application of the present model for different casting conditions. All the input parameters for the model such as surface roughness, temperatures, pressure, etc were taken from these reported experimental measurements. Their values are presented in the table integrated into the following figures for the purpose of accuracy.

One of the interesting findings in the present analysis is the contribution of the alloy composition through its density and latent heat and the casting thickness to the evolution of *h(t)* during solidification (see Equation (25)), although these properties do not appear in the first stage of contact when *h* is at its peak value (see Equation (13)). Fortunately, the authors of this paper have experimentally determined the *h(t)* for two different alloys, AZ91D and Al-9Si-3Cu, which have a different latent heat and density (see reference [12,14]). We have also tested different thicknesses of the castings. This provides the context for an effective comparison and validation of the model.

Fig. 5 shows the variation of the modelled *h* at the casting–die interface with time for both AZ91D and Al-9Si-3Cu alloys compared to the experimentally determined evolution of *h(t)* reported for both AZ91D and Al-9Si-3Cu alloys. The two curves *h(model)* and *h(experimental)* for both alloys are in good agreement. They exhibit the same trends versus time. In addition, the modelled and experimentally determined *h(t)* shows almost the same trend with the drop of *h(t)* in the case of AZ91D alloy sharper than with the Al-9Si-3Cu alloy.

Furthermore, in Fig. 6, the experimental *h(t)* at the casting–die interface for two different casting thicknesses (2 mm and 4 mm) are plotted as a function of time for the AZ91D alloy. They are also compared to those calculated from the model for the 2 mm and 4 mm thickness castings. As can be seen in the figures, the experimentally determined and the calculated *h(t)* values have similar trends versus time along with similar orders of magnitude. For both the modelled and experimentally measured *h(t)*, the drop of *h(t)* with time is sharper for the thinner casting.

4. Discussion

There is good agreement between the model and the experimental measurements. This agreement confirms the relevance of our theoretical approach: the arguments used are reasonable descriptions of the elements that contribute to the creation of the

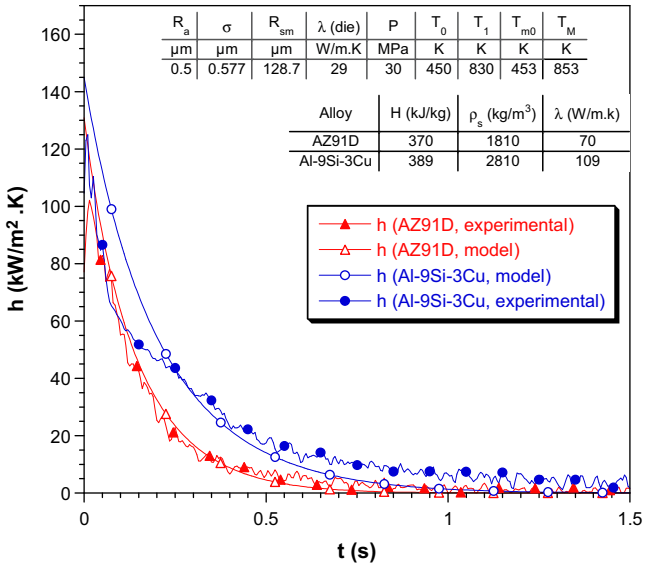

Fig. 5. Modelled and experimentally determined of the Evolution of h as a function of time for both AZ91D and Al-9Si-3Cu alloys.

peak value and the transitory phase of *h* during solidification of metal in HPDC process. The results show that the peak value of *h* in HPDC is governed by the contact topography and the mechanisms of contact (pressure balance between the liquid, entrapped air and surface tension). As for, the variation of *h* with time it is mostly determined by the properties and geometry of the alloy that is cast along with the nature of the phase changes that take place in the casting during solidification.

The agreement between the sets of curves further confirms that the drop in the *h(t)* is due to the reduction of the number and the radius of contact spots between the casting and the die during solidification as interpreted elsewhere by Loulou [20] from his experimental analysis. In order to highlight this issue, a_s and n_s have been plotted in Fig. 7 as a function of time for the case of contact between the AZ91D alloy and the die (H11). As shown, a_s and n_s reach their minimum values (around zero) at around 1.5 s but the

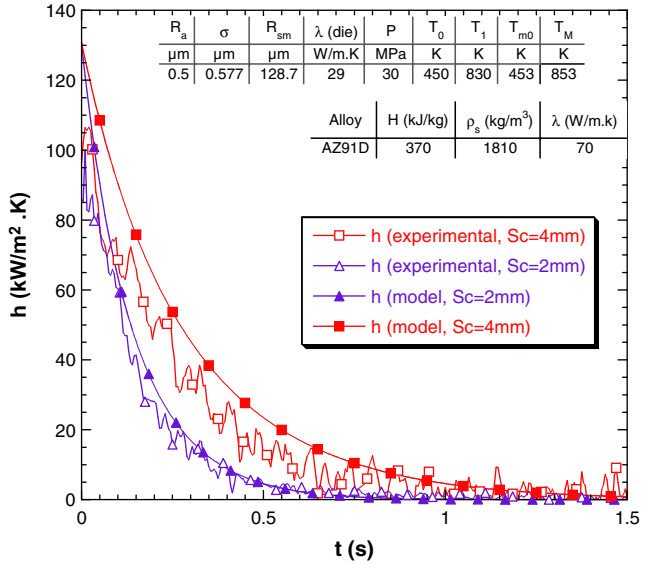

Fig. 6. Comparison between experimental and modelled h versus time for two different casting thicknesses 2 mm and 4 mm.

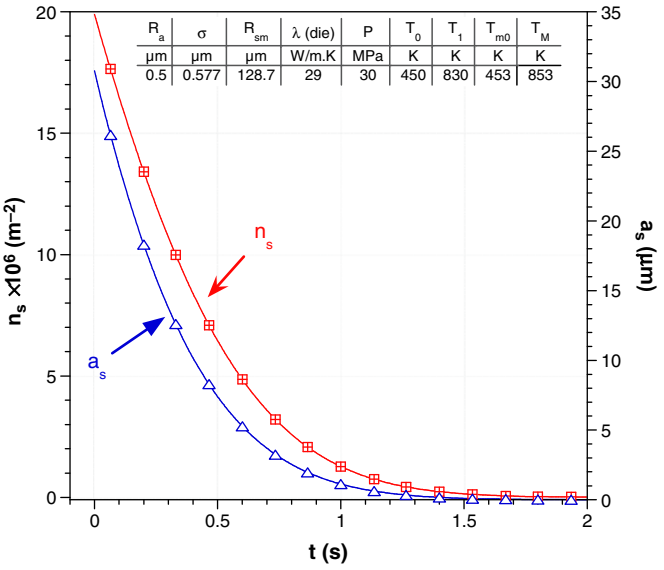

Fig. 7. The variation of as and ns with time in the case of HPDC of Al-9Si-3Cu alloy.

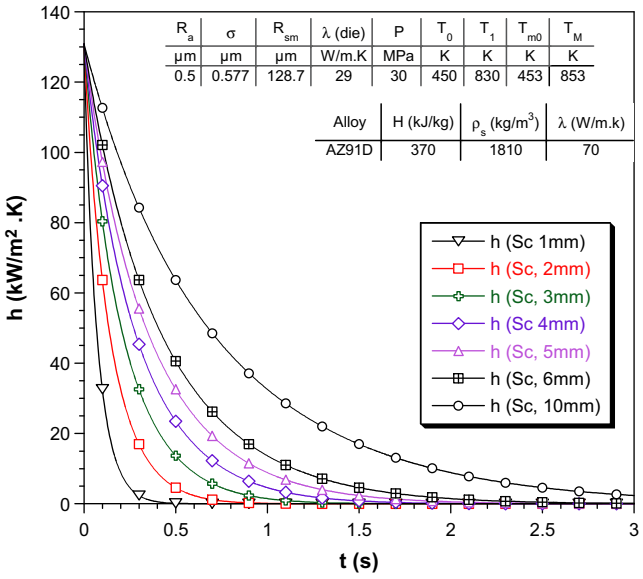

Fig. 9. Variation of h as a function of time as predicted for different casting thicknesses, in HPDC.

$h(t)$ reaches its minimum value after around one second. This means that at 1 s the contact between the casting and the die is completely transformed to solid–solid contact. Even under this situation of solid–solid contact any pressure applied to the casting should be transmitted to the die surface, hence, there are still a very small number of microcontact areas where $h(t)$ is around zero. It is only after 1.5 s that n_s and a_s drop to a zero value. At this time an air gap is expected to form at the interface because of the global shrinkage across its solidified thickness.

It is also worth noting that the drop in the experimental and modelled $h(t)$ has a sharper slope for the AZ91D alloy compared to that present in the case of the Al-9Si-3Cu alloy. This is logical since the low density and latent heat of the AZ91D alloy means that the heat absorbed by the die during solidification of the AZ91D alloy is small, compared to that of the Al-9Si-3Cu alloy. As a result, the solidification time of the AZ91D alloy is shorter than that of the Al-9Si-3Cu alloy for the same set of casting conditions. As solidification becomes more rapid, the faster the contraction and the faster a_s and n_s decrease resulting in a sharper drop of the $h(t)$ curve. These results are also consistent with the conclusions reported in reference [23] that deals with the effect of alloy type on the variation of the thermal contact resistance (R) with time. Fig. 8 shows the experimental results of the evolution of R vs. time for Tin, Lead and Zinc as reported in the mentioned reference. It has been concluded that the cooling rate is strongly related to the volumic latent heat of the material which is undergoing solidification. For this reason the R curve for Lead decreases more rapidly than the R curves for Tin and Zinc which have a greater latent heat.

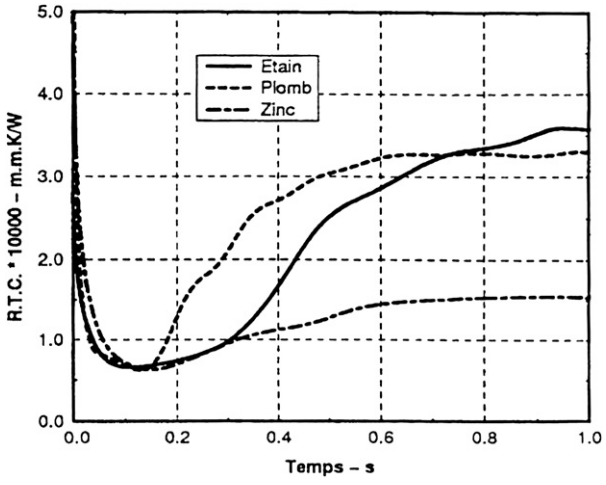

Fig. 8. Thermal contact resistance substrate-Tin (Etain), Lead (Plomb) and Zinc interstitial fluid: air [23].

As for the effect of casting thickness on $h(t)$, it would seem reasonable to relate it to the casting volume. The thicker casting is associated with a larger volume of cast alloy which is associated with a larger total latent heat to be absorbed. Thus, the time needed to extract the larger amount of latent heat becomes more important, if values for h_o during the first stage of solidification are identical (the same conditions of the casting process and contact between the casting and the die). Consequently, the time for $h(t)$ to fall to its minimum value increases. Hence, the slope of the $h(t)$ curve becomes smaller for the larger thickness castings.

In addition to the contribution of the present analysis in the understanding of the mechanisms of the transitory $h(t)$ or $R(t)$ at the liquid–solid interface in general, the model also provides a valuable tool for investigators to understand the effect of various casting process parameters, die surface roughness, casting quality and thickness on the $h(t)$ during the HPDC process. These results should be considered as a departure point directing the investigations towards modelling the solidification time in HPDC as a function of the casting–die contact conditions. As the model shows that the slope of the drop in $h(t)$ should increase regularly with casting thickness as shown in Fig. 9 or with casting volume. Thus, it should be possible to relate the time of solidification to these slopes. This requires further experimental validation using a wide range of casting thicknesses and materials.

5. Conclusion

An analytical approach has been proposed to model the transitory thermal conductance ($h(t)$) at the casting–die interface in HPDC. The approach is based on a model which includes the initial conditions of both the topography and contact mechanisms between casting and its die and then incorporates the degradation

of this contact with time as it is thought to occur as the solidification of the casting progresses.

The degradation of contact has been related to the increase in the separation plane between the casting and the die during solidification which results in a decrease in the area and the density of micro-contact points.

The results of the model show good agreement with the available experimental data for different alloys and casting thickness.

It has also been shown that that the peak value of the thermal conductance is primarily determined by both the topography and the mechanisms of contact between the casting and the die, whereas, the transitory phase of $h(t)$ is further governed by the geometry and composition of casting.

Acknowledgments

The authors acknowledge CROUS, Ecole des Mines d'Albi Carmaux, the University of Queensland and the CAST Cooperative Research Centre for supporting this activity including a Co-tutelle agreement between the Université Paul Sabatier and the University of Queensland.

References

[1] M.S. Dargusch, G. Dour, N. Schauer, C.M. Dinnis, G. Savage, The influence of pressure during solidification of high pressure die cast aluminium telecommunications components, J. Mater. Process. Technol. 180 (1–3) (2006) 37–43.
[2] N. El-Mahallawy, A. Taha Mohamed, E. Pokora, F. Klein, On the influence of process variables on the thermal conditions and properties of high pressure die–cast magnesium alloys, J. Mater. Process. Technol. 73 (1–3) (1998) 125–138.
[3] Z.W. Chen, Skin solidification during high pressure die casting of Al-11si-2cu-1fe alloy, Mater. Sci. Eng. A 348 (1–2) (2003) 145–153.
[4] S.G. Lee, G.R. Patel, A.M. Gokhale, Characterization of the effects of process parameters on macrosegregation in a high-pressure die–cast magnesium alloy, Mater. Charact. 55 (3) (2005) 219–224.
[5] S.G. Lee, A.M. Gokhale, Formation of gas induced shrinkage porosity in Mg-alloy high-pressure die–castings, Scr. Mater. 55 (4) (2006) 387–390.
[6] H. Yamagata, W. Kasprzak, M. Aniolek, H. Kurita, J.H. Sokolowski, The effect of average cooling rates on the microstructure of the Al-20% Si high pressure die casting alloy used for monolithic cylinder blocks, J. Mater. Process. Technol. 203 (1–3) (2008) 333–341.
[7] C.M. Gourlay, H.I. Laukli, A.K. Dahle, Defect band characteristics in Mg–Al and Al–Si high-pressure die castings, Metall. Mater. Trans. A 38 (8) (2007) 1833–1844.
[8] M.F. Horstemeyer, N. Yang, K. Gall, D.L. Mcdowell, J. Fan, P.M. Gullett, High cycle fatigue of a die cast Az91e-T4 magnesium alloy, Acta Mater. 52 (5) (2004) 1327–1336.
[9] D.J.F.A. Kurz, Fundamentals of Solidification Netherlands ed, Trans Tech Publications SA, Switzerland, 1984.
[10] M. Prates, H. Biloni, Variables affecting the nature of the chill zone, Metall. Trans. 3 (1972) 1501–1510.
[11] G. Dour, Fonderie-Aide-Mémoire, Dunod, Paris, 2004.
[12] A. Hamasaiid, G. Dour, M. Dargusch, T. Loulou, C. Davidson, G. Savage, Heat-transfer coefficient and in-cavity pressure at the casting–die interface during high-pressure die casting of the Magnesium Alloy Az91d, Metall. Mater. Trans. A 39 (4) (2008) 853–864.
[13] G. Dour, M. Dargusch, C. Davidson, A. Nef, Development of a non-intrusive heat transfer coefficient gauge and its application to high pressure die casting: effect of the process parameters, J. Mater. Process. Technol. 169 (2) (2005) 223–233.
[14] M.S. Dargusch, A. Hamasaiid, G. Dour, T. Loulou, C. Davidson, D.H. St John, The accurate determination of heat transfer coefficient and its evolution with time during high pressure die casting of Al-9%Si-3%Cu and Mg-9%Al-1%Zn Alloys, Adv. Eng. Mater. 9 (13) (2008) 995–999.
[15] A. Hamasaiid, G. Dour, M. Dargusch, T. Loulou, C. Davidson, G. Savage, Heat transfer at the casting/die interface in high pressure die casting—experimental results and contribution to modelling, in: Modeling of Casting, Welding, and Advanced Solidification XI, TMS, 2006, pp. 1213–1216.
[16] H. Fujimoto, H. Shiraishi, N. Hatta, Evolution of liquid/solid contact area of a drop impinging on a solid surface, Int. J. Heat Mass Transfer 43 (9) (2000) 1673–1677.
[17] S. Chandra, C.T. Avedisian, On the collision of a droplet with a solid surface, Proc. R. Soc. Lond. A 432 (1991) 13–41.
[18] M. Rein, Phenomena of liquid drop impact on solid and liquid surfaces, Fluid Dyn. Res. 12 (2) (1993) 61–93.
[19] R.S. Timsit, The true area of contact between a liquid and a rough solid: elementary considerations, Wear 83 (1) (1982) 129–141.
[20] T. Loulou, Etude Expérimentale de l'Evolution des Conditions Thermiques de Contact Lors de la Solidification d'un Métal Tombant sur une Paroi Métallique, PhD thesis, Université de Nantes, Nantes, 1995.
[21] M. Leigh, Surface Texture Analysis: The Handbook, Hommelwerke GmbH, Mühlhausen, 1992.
[22] M. G Cooper, B.B. Mikic, M.M. Yovanovich, Thermal contact conductance, Int. J. Heat Mass Transfer 12 (3) (1969) 279–300.
[23] T. Loulou, E.A. Artyukhin, J.P. Bardon, Estimation of thermal contract resistance during the first stages of metal solidification process: Ii–experimental setup and results, Int. J. Heat Mass Transfer 42 (12) (1999) 2129–2142.
[24] M. Prates, H. Biloni, Variables affecting the nature of the chill Zone, Metall. Transfer 3 (6) (1972) 1501–1510.
[25] A. Hamasaiid, Interfacial Heat Transfer in Die Casting of Light Alloys, Ph.D thesis, Université Paul Sabatier (France) and University of Queensland (Australia), Brisbane, Albi, 2007.
[26] G. Dour, M. Dargusch, C. Davidson, Recommendations and guidelines for the performance of accurate heat transfer measurements in rapid forming processes, Int. J. Heat Mass Transfer 49 (11–12) (2006) 1773–1789.